EPJ A
Hadrons and Nuclei

EPJ.org
your physics journal

Eur. Phys. J. A (2011) **47**: 80 DOI: 10.1140/epja/i2011-11080-9

Polarized electric dipole moment of well-deformed reflection asymmetric nuclei

V.Yu. Denisov

EDP SCIENCES Società Italiana di Fisica Springer

Eur. Phys. J. A (2011) **47**: 80
DOI 10.1140/epja/i2011-11080-9

THE EUROPEAN PHYSICAL JOURNAL A

Regular Article – Theoretical Physics

Polarized electric dipole moment of well-deformed reflection asymmetric nuclei

V.Yu. Denisov[a]

Institute for Nuclear Research, Prospect Nauki 47, 03680 Kiev, Ukraine

Received: 17 February 2011 / Revised: 7 April 2011
Published online: 21 June 2011 –
Communicated by J. Wambach

Abstract. The expression for polarized electric dipole moment of well-deformed reflection asymmetric nuclei is obtained in the framework of the liquid-drop model in the case of geometrically similar proton and neutron surfaces. The expression for polarized electric dipole moment consists of the first- and second-order terms. It is shown that the second-order correction terms of the polarized electric dipole moment are important for well-deformed nuclei.

1 Introduction

The reflection asymmetric deformation of the nucleus induces proton-neutron redistribution. As a result, the proton or neutron density distributions become slightly polarized and reflection asymmetric in the nuclear volume. Due to such density polarization the position of the proton center of mass is shifted relatively to the nuclear center of mass; therefore reflection asymmetric nuclei have polarized electric dipole moment (PEDM).

The PEDM of nuclei with quadrupole and octupole surface deformations was firstly obtained by V.M. Strutinsky in 1956 [1] in the framework of the liquid-drop model. A short time later A. Bohr and B.R. Mottelson evaluated the PEDM in the same model [2], but Strutinsky's derivation is the correct one [3]. The PEDM was found for non-axial nuclei with quadrupole and octupole deformations in refs. [4,5]. Note that the PEDM discussed in refs. [1–5] is only related to the proton-neutron polarization in the volume of nuclei with quadrupole and octupole surface deformations.

However, the proton-neutron density polarization in the nuclear volume induces the variation of proton and neutron radii and, therefore, leads to the corresponding surface contribution into the PEDM. The expression for PEDM with volume and surface contributions was derived in ref. [6] in the framework of the droplet model for axial nuclei with the proton radius $R_p(\theta)$ in the form

$$\frac{R_p(\theta)}{R_{0p}} = F(\theta) = \left[1 + \sum_{\ell=2}^{L} \beta_\ell Y_{\ell 0}(\theta)\right]. \qquad (1)$$

Here R_{0p} is the proton radius of the spherical nucleus, β_ℓ is the deformation parameter and $Y_{\ell 0}(\theta)$ is the spherical harmonic function. Both spherical and deformed nuclei have a neutron skin of constant thickness in the framework of the droplet model, see ref. [6] and papers cited therein, therefore the neutron radius, $R_n(\theta)$, of deformed nuclei is not proportional to the proton one, $R_p(\theta)$, in the droplet model. Due to this, the expression for the PEDM obtained in the droplet model consists of the volume and surface charge redistribution contributions as well as the contribution related to the neutron skin thickness [6,7]. The neutron skin thickness contribution arises precisely from the non-coincidence of the centers of mass of a uniform skin and of the volume it encloses [6,7].

The expression for PEDM for nuclei with geometrically similar proton and neutron surfaces, *i.e.* when proton and neutron radii have the same angular dependence,

$$\frac{R_p(\theta)}{R_{0p}} = \frac{R_n(\theta)}{R_{0n}} = F(\theta), \qquad (2)$$

was obtained in ref. [8]. Here R_{0n} is the neutron radius of the spherical nucleus. The neutron skin thickness depends on θ, when the radii of the proton and neutron surfaces are proportional to each other. The PEDM consists of the volume and surface charge redistribution contributions only in this case [8], because the neutron skin thickness contribution equals zero for geometrically similar proton and neutron surfaces, see for details [7–9] and sect. 2. The neutron skin center of mass coincides with the nucleus one [8,9].

The expressions for volume and surface parts of the PEDM for non-axial nuclei with arbitrary multipole deformations and geometrically similar proton and neutron surfaces are given in ref. [10]. The equilibrium shapes of some nuclei are non-axial reflection asymmetric [11]. Moreover, PEDM can arise at non-axial reflection asymmetric surface vibrations [10].

[a] e-mail: denisov@kinr.kiev.ua

We emphasize that the PEDM obtained in the first non-zero order on multipole deformations of nuclear surface is proportional to $\beta_\ell\beta_{\ell+1}$ and all the expressions for the PEDM presented in refs. [1–10] are derived in this approximation.

The numerical study of the PEDM in well-deformed nuclei in ref. [12] shows that the first approximation for the PEDM is strongly underestimated with respect to the numerical one. Moreover, the difference between the numerical and first-order values of PEDM increases with the values of deformation parameters strongly [12].

The values of PEDM have been also evaluated in the frameworks of various semi-microscopic or microscopic approaches, see refs. [9,12–16] and papers cited therein.

Nuclei with quadrupole and octupole deformations, $E1$ transitions and the PEDM have been studied intensively recently [17–26]. The PEDM plays an important role in various phenomena of well-deformed reflection asymmetric nuclei. Thus Karpeshin has shown that well-deformed fission fragments of such shapes formed during prompt fission give rise to both the anomalous $E1$ internal conversion [27] and the prompt gamma radiation [28,29] related to the PEDM. The left-right asymmetry of the fission induced by polarized neutrons can be also linked to the PEDM [30]. The $E1$ transitions possibly linked to octupole vibrations around super-deformed shape can be also enhanced by the PEDM [31–35]. Strong $E1$ transitions related to the low-energy shape oscillations of negative parity in the first and second (isomeric) minima in actinides are also connected to the PEDM [36].

However the application of the expression for the PEDM obtained in the first order for well-deformed nuclei is questionable as pointed out by Skalski [12]. Therefore, it is desirable to obtain an expression for the PEDM in the next order at least, which is the second-order approximation for the PEDM contained terms proportional to $\beta_\ell\beta_{\ell'}\beta_{\ell''}$. Such expression should be helpful and practical for the description of the various nature of the $E1$ transition in well-deformed nuclei.

The PEDM evaluated in the framework semi-microscopic approaches [13,14] consists of macroscopic and microscopic contributions. The microscopic contribution of PEDM is evaluated without applying the perturbation approach on the surface deformation parameters, while the macroscopic one is evaluated by using the expressions obtained in the first non-zero order on multipole deformations. Therefore a more accurate expression for the macroscopic part of the PEDM improves the accuracy of the PEDM evaluated in the framework of semi-microscopic models.

It is well known that shell effects are reduced in heated nuclei. Due to this, the expression for PEDM has reliable accuracy for highly excited fission fragments. The shape of fission fragments after the rupture has an appreciable reflection asymmetry. The microscopic calculation of PEDM in heated nuclei has not been done up to now. Therefore the expression for the PEDM obtained in the next order can at least be useful for the evaluation of the various effects related to the dipole moment of fission fragments.

Various proposals on neutron skin are discussed recently. The neutron skin of permanent thickness in deformed nuclei is widely applied in the framework of the droplet model ([6,7] and other papers related to this model). The neutron skin with thickness depending on θ and related to the well-known and widely used relation for the proton and neutron radii (2) is also very common in nuclear physics; see, for example, the description of the proton and neutron mean field radii etc. [9,12,14,37–44]. We emphasize that the shapes of potential and density distributions are geometrically similar due to a consistency between the density distribution and the corresponding mean-field potential [9]. A more complex approximation to the neutron skin thickness related to different neutron *versus* proton deformations of nuclei is discussed in refs. [45,46]. The thickness of the neutron skin has a complex angular dependence on θ in that case.

Diverse approximations for the neutron skin shape are reasonable for small and medium deformed nuclei close to the beta-stability line. The ratio (2) between the proton and neutron radii is, probably, discussable for extremely deformed and/or neutron-rich nuclei as pointed out in ref. [7]. Current experimental studies of neutron distribution on the surface of nuclei are devoted to the neutron skin thickness in spherical nuclei mainly (see refs. [47, 48] and papers cited therein). The available experimental data [47,48] cannot support firmly any of these approximations on the neutron skin thickness in deformed nuclei.

The relationship between proton and neutron surfaces or the potential described by eq. (2) is very widely used in nuclear physics for small, medium and even well-deformed nuclei [9,12,14,37–44]. Therefore, in sect. 2 we derive the expressions for the PEDM for the geometrically similar proton and neutron surfaces, which take into account the first ($\propto \beta_\ell\beta_{\ell+1}$) and second ($\propto \beta_\ell\beta_{\ell'}\beta_{\ell''}$) orders contributions. Discussion of the obtained expressions, numerical results and conclusions are given in sect. 3.

2 Model and expression for the PEDM

Let us consider the axial nucleus with proton and neutron radii described by eq. (2). There are no density polarizations in spherical nuclei, therefore the equilibrium neutron and proton density distributions in deformed nucleus can be presented as $\rho_n = \rho_{0n} + \delta\rho_n$ and $\rho_p = \rho_{0p} + \delta\rho_p$. Here $\rho_{0n} = 3N/(4\pi R_{0n}^3)$ and $\rho_{0p} = 3Z/(4\pi R_{0p}^3)$ are the equilibrium neutron and proton densities in the spherical nucleus, $\delta\rho_n$ and $\delta\rho_p$ are the variations of neutron and proton densities induced by surface deformation, Z and N are the numbers of protons and neutrons in the nucleus.

Due to the high value of nuclear matter incompressibility, the total nuclear density $\rho = \rho_n + \rho_p$ in the nuclear volume is constant $\rho = \rho_{0n} + \rho_{0p}$, therefore $\delta\rho_n = -\delta\rho_p$ (see also [1,8]).

We should take into account that the numbers of protons and neutrons in deformed nucleus are, respectively, Z and N; the center of mass must lie in the plane of mirror symmetry of the nucleus [1,8,9], because the reflection

asymmetric nuclear shapes are coupled by a sub-barrier tunnel transition. These two conditions can be easy fulfilled by the introduction of auxiliary monopole β_0 and dipole β_1 deformations, *i.e.*

$$\frac{R_p(\theta)}{R_{0p}} = \frac{R_n(\theta)}{R_{0n}} = F(\theta) + \beta_0 Y_{00}(\theta) + \beta_1 Y_{10}(\theta) = f(\theta) = 1 + \sum_{\ell=0}^{L} \beta_\ell Y_{\ell 0}(\theta). \quad (3)$$

The values of β_0 and β_1 are, correspondingly, determined by the equations

$$\int \mathrm{d}V \frac{\rho_{0p}}{Z} = \int \mathrm{d}V \frac{\rho_{0n}}{N} = \frac{1}{2}\int_0^\pi \mathrm{d}\theta \sin(\theta) f(\theta)^3 = 1, \quad (4)$$

$$\int \mathrm{d}V\ r\cos(\theta)(\rho_{0p} + \rho_{0n}) = \frac{3}{8}(ZR_{0p} + NR_{0n}) \times \int_0^\pi \mathrm{d}\theta\ \sin(\theta)\cos(\theta) f(\theta)^4 = 0. \quad (5)$$

For the sake of simplicity we take into account the most important multipole deformations of the nuclear surface β_2, β_3, β_4, β_5, β_6. The expressions for β_0 and β_1 taking into account all quadratic and cubic terms on β_2, β_3, β_4, β_5, β_6 can be directly obtained from eqs. (4) and (5), however the corresponding equations are cumbersome and therefore not presented here.

The PEDM is defined as

$$D \equiv e\int \mathrm{d}V\ r\cos(\theta)\rho_p. \quad (6)$$

Due to the deviation of the nuclear surface from the spherical form there are variations of the proton density in the nuclear volume $\delta\rho_p(\mathbf{r})$. The variation of nucleon density in the nuclear volume induces the deviation of the proton radius $\delta R_p(\theta)$ from the equilibrium position on the nuclear surface. The proton radius variation induces proton density variations in the volume $\delta R_p(\theta)\Delta\mathcal{S}$, where ΔS is the element of surface square. Therefore, the PEDM in reflection asymmetric nuclei with axial symmetry is related to the redistribution of protons relatively to neutrons in the nuclear volume and on the nuclear surface (see also [6,8]),

$$D = D_v + D_s, \quad (7)$$

where

$$D_v \approx e\int \mathrm{d}V r\cos(\theta)[\rho_{0p} + \delta\rho_p] = e\int \mathrm{d}V r\cos(\theta)\delta\rho_p = 2\pi e\int_0^\pi \mathrm{d}\theta\ \sin(\theta)\cos(\theta)\int_0^{R_{0p}f(\theta)} \mathrm{d}r\ r^3\delta\rho_p, \quad (8)$$

$$D_s \approx e\int \mathrm{d}\mathcal{S}\ R_p(\theta)\cos(\theta)\ \rho_{0p}\ \delta R_p(\theta) = \frac{3Ze}{2}\int_0^\pi \mathrm{d}\theta \sin(\theta)\cos(\theta)\left[1 + \left(\frac{f'(\theta)}{f(\theta)}\right)^2\right]^{1/2} \times f^3(\theta)\delta R_p(\theta). \quad (9)$$

Here eq. (5) is taken into account upon simplification of eq. (8) and $f'(\theta) = \frac{\mathrm{d}f(\theta)}{\mathrm{d}\theta}$. So, the volume part of the PEDM is related to the volume integral and density variation in the nuclear volume $\delta\rho_p$ while the surface part is determined by the surface integral and the proton radius variation $\delta R_p(\theta)$.

The proton (or neutron) density variation induced by surface deformation produces additional pressure on the free nuclear surface. Due to this pressure, the position of the corresponding surface is slightly shifted. Both the surface symmetry energy and the Coulomb force counteract the surface shift and neutralize the additional pressure on the free nuclear surface induced by density variations, see for details [6,8,10]. The normal to the surface variation of the proton radius is defined by the boundary condition [6, 8,10], which equalizes the normal to surface pressures induced by density fluctuations, neutron-skin stiffness and the Coulomb interaction, and is equal to

$$\delta R_p(\theta) = -\frac{N}{A}\frac{3eR_0}{8QA^{1/3}}\left[\phi(R_p(\theta)) - \frac{\int \mathrm{d}\mathcal{S}\phi(R_p(\theta))}{\int \mathrm{d}\mathcal{S}}\right] = -\frac{N}{A}\frac{3eR_0}{8QA^{1/3}}\left[\varphi(R_p(\theta)) - \frac{\int \mathrm{d}\mathcal{S}\varphi(R_p(\theta))}{\int \mathrm{d}\mathcal{S}}\right], \quad (10)$$

where Q is the neutron-skin stiffness coefficient [6,10], $\phi = \varphi - \overline{\varphi}$, $\varphi(\mathbf{r})$ is the Coulomb potential related to the protons, $\overline{\varphi} = \frac{\int \mathrm{d}V\varphi}{\int \mathrm{d}V}$ is the average potential value in the nucleus and $A = Z+N$. Note that $Z\delta R_p(\theta) + N\delta R_n(\theta) = 0$, because the center of the mass must lie in the plane of mirror symmetry of the nucleus, *i.e.*

$$\begin{aligned}
&\int \mathrm{d}V\ r\cos(\theta)\ \rho(\mathbf{r}) \\
&= \int \mathrm{d}V\ r\cos(\theta)\ [\rho_{0p} + \delta\rho_p + \rho_{0n} + \delta\rho_n] \\
&\quad + \int \mathrm{d}\mathcal{S}\ \cos(\theta)\ [R_p(\theta)\rho_{0p}\delta R_p + R_n(\theta)\rho_{0n}\delta R_n] \\
&= \int \mathrm{d}V\ r\cos(\theta)\ [\delta\rho_p + \delta\rho_n] \\
&\quad + \int \mathrm{d}\mathcal{S}\ \cos(\theta)\ [R_p(\theta)\rho_{0p}\delta R_p + R_n(\theta)\rho_{0n}\delta R_n] \\
&= \int \mathrm{d}\mathcal{S}\ \cos(\theta)\ [R_p(\theta)\rho_{0p}\delta R_p + R_n(\theta)\rho_{0n}\delta R_n] \\
&\quad \approx \int \mathrm{d}\mathcal{S}\ \cos(\theta)\ R_p(\theta)[\rho_{0p}\delta R_p + \rho_{0n}\delta R_n] = 0.
\end{aligned}$$

Here eq. (5) and the condition $\delta\rho_p = -\delta\rho_n$ are taken into account.

If we know $\delta\rho_p(\mathbf{r})$ and $\varphi(\mathbf{r})$ than we can evaluate the PEDM using eqs. (7)–(10). Let us find $\delta\rho_p(\mathbf{r})$ and $\varphi(\mathbf{r})$ in the framework of the liquid-drop model. The energy density functional, which describes the density distribution in the nuclear volume, can be written in a simple

form [1,8,10]

$$\mathcal{E} \approx -a_v\rho + J\frac{(\rho_n-\rho_p)^2}{\rho} + e\rho_p\varphi = -a_v\rho + J\frac{(\rho-2\rho_p)^2}{\rho} + e\rho_p\varphi, \quad (11)$$

where $-a_v$ is the bulk energy per nucleon in symmetric nuclear matter and J is the volume symmetry energy. Note that the energy density functional of the droplet model contains the dilatation term [6], but the parameter L related to the dilatation term is equal to zero in the recent parameter set of the droplet model [6], therefore we neglect the dilatation term here. The nucleus energy E is related to the energy density functional $E = \int \mathrm{d}V\mathcal{E}$. The equation determining the equilibrium distribution of the charge in the nuclear volume can be obtained by the variation of the energy

$$\delta E = \delta\int \mathrm{d}V\,[\mathcal{E} - \lambda\rho_p] = \int \mathrm{d}V\,[-4J(\rho-2\rho_p)/\rho + e\varphi - (a_v+\lambda)]\,\delta\rho_p, \quad (12)$$

in $\delta\rho_p$ with the additional condition of number of proton conservation in the nucleus. As a result, we get

$$8J\rho_p = -\rho(e\varphi - 4J - \lambda'), \quad (13)$$

where $\lambda' = a_v + \lambda$ and λ is the Lagrangian coefficient related to the additional condition. The solution of this equation is

$$\rho_{0p} = \rho\left(\frac{1}{2} + \frac{\lambda'}{8J} - \frac{e\overline{\varphi}}{8J}\right) = (\rho_{0p}+\rho_{0n})\left(\frac{1}{2} + \frac{\lambda'}{8J} - \frac{e\overline{\varphi}}{8J}\right), \quad (14)$$

$$\delta\rho_p = \frac{-e\rho(\varphi-\overline{\varphi})}{8J} = \frac{-e(\rho_{0p}+\rho_{0n})(\varphi-\overline{\varphi})}{8J} = \frac{-3eA(\varphi-\overline{\varphi})}{32\pi R_{0p}^3 J} = \frac{-3eA\phi}{32\pi R_{0p}^3 J}\,. \quad (15)$$

Note that $\int \mathrm{d}V\delta\rho_p = \frac{-3eA}{32\pi R_{0p}^3 J}\big[\int \mathrm{d}V(\varphi-\overline{\varphi})\big] = 0$. We neglect the difference between R_{0p} and R_{0n} at the evaluation of volume quantities.

The electric potential can be found by using the Poisson equation

$$\nabla^2\varphi = 4\pi e\rho_p. \quad (16)$$

Substituting (15) into (8) and taking into account (5) we get

$$D_v \approx \frac{-3e^2A}{16JR_{0p}^3}\int_0^\pi \mathrm{d}\theta\,\sin(\theta)\cos(\theta)\int_0^{R_{0p}f(\theta)} \mathrm{d}r\,r^3\phi(\mathbf{r}) = \frac{-3e^2A}{16JR_{0p}^3}\int_0^\pi \mathrm{d}\theta\,\sin(\theta)\cos(\theta)\int_0^{R_{0p}f(\theta)} \mathrm{d}r\,r^3\varphi(\mathbf{r}). \quad (17)$$

Using (10) and the approximation $\frac{NZ}{A} \approx \frac{A}{4}$, see ref. [6], we rewrite (9) in the form

$$D_s \approx -\frac{9Ae^2R_0}{64QA^{1/3}}\int_0^\pi \mathrm{d}\theta\; g(\theta)\cos(\theta)f(\theta) \times\left[\varphi(R_p(\theta)) - \frac{\int_0^\pi \mathrm{d}\theta'\; g(\theta')\varphi(R_p(\theta'))}{\int_0^\pi \mathrm{d}\theta'\; g(\theta')}\right], \quad (18)$$

where $g(\theta) = \sin(\theta)f^2(\theta)[1+(f'(\theta)/f(\theta))^2]^{1/2}$. So, the volume (17) and surface (18) parts of PEDM are determined by the Coulomb potential $\varphi(\mathbf{r})$.

The Coulomb potential of the deformed nucleus is

$$\varphi(\mathbf{r}) = e\int \mathrm{d}V\frac{\rho_p(\mathbf{r}')}{|\mathbf{r}-\mathbf{r}'|} = e\int \mathrm{d}V\frac{\rho_{0p}+\delta\rho_p(\mathbf{r}')}{|\mathbf{r}-\mathbf{r}'|}\,. \quad (19)$$

This potential satisfies eq. (16).

It is possible to find the potential $\varphi(\mathbf{r})$ by applying the perturbation theory to eqs. (14), (15) and (19). We expand the potential and the variation of proton density into the perturbation series

$$\varphi(\mathbf{r}) = \varphi^0(\mathbf{r}) + \varphi^1(\mathbf{r}) + \varphi^2(\mathbf{r}) + \ldots, \quad (20)$$

$$\delta\rho_p(\mathbf{r}) = \delta\rho_p^0(\mathbf{r}) + \delta\rho_p^1(\mathbf{r}) + \delta\rho_p^2(\mathbf{r}) + \ldots, \quad (21)$$

where the superscript corresponds to the number-of-perturbation approach. The corresponding solution for the Lagrangian coefficient is the variation of proton density into the perturbation series

$$\lambda = -a_v + 8J\Big[Z/A - 1/2 + e/(8J)\Big(\overline{\varphi^0(\mathbf{r})} + \overline{\varphi^1(\mathbf{r})} + \overline{\varphi^2(\mathbf{r})} + \ldots\Big)\Big].$$

Substituting the perturbation series (20)-(21) into eqs. (15) and (19) we get

$$\delta\rho_p^k(\mathbf{r}) = \frac{-e\rho\phi^k(\mathbf{r})}{8J} = \frac{-3eA\phi^k(\mathbf{r})}{32\pi R_{0p}^3 J}\,, \qquad \text{for } k\geq 0, \quad (22)$$

$$\varphi^k(\mathbf{r}) = e\int \mathrm{d}V\frac{\delta\rho_p^{k-1}(\mathbf{r}')}{|\mathbf{r}-\mathbf{r}'|}\,, \qquad \text{for } k\geq 1, \quad (23)$$

and

$$\varphi^0(\mathbf{r}) = e\int \mathrm{d}V\frac{\rho_{0p}}{|\mathbf{r}-\mathbf{r}'|} = \frac{eZ}{R_{0p}}\int \mathrm{d}V\frac{3}{4\pi R_{0p}^2|\mathbf{r}-\mathbf{r}'|} = \frac{eZ}{R_{0p}}\sum_\ell \frac{6\pi Y_{\ell 0}(\theta)}{(2\ell+1)}\int_0^\pi \mathrm{d}\theta'\sin(\theta')Y_{\ell 0}^*(\theta') \times\left[\int_0^r \mathrm{d}r'\frac{(r')^{\ell+2}}{r^{\ell+1}(R_{0p})^2} + \int_r^{R_{0p}f(\theta')} \mathrm{d}r'\frac{(r)^\ell}{(r')^{\ell-1}(R_{0p})^2}\right], \quad (24)$$

where $\phi^k(\mathbf{r}) = \varphi^k(\mathbf{r}) - \overline{\varphi^k(\mathbf{r})}$.

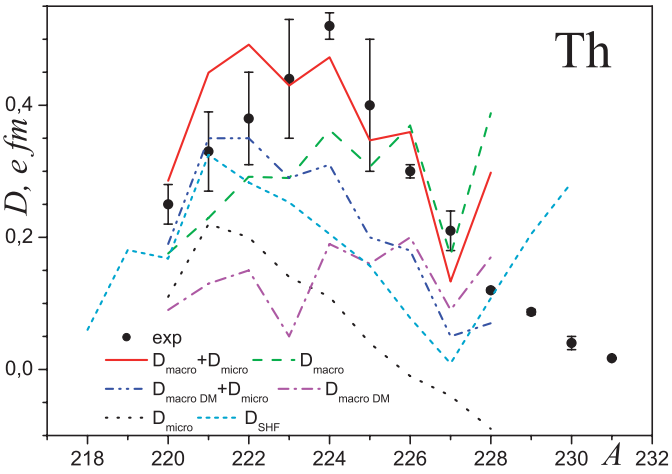

Fig. 1. Experimental and theoretical values of the PEDM as well as macroscopic and microscopic contributions to the PEDM for Th isotopes. Points are experimental data from refs. [13,25,26]. For details on theoretical lines see the text.

Using eqs. (22) and (23) we get the recurrent equation for $\varphi^k(\mathbf{r})$ at $k \geq 1$

$$\varphi^k(\mathbf{r}) = \frac{-3e^2A}{32\pi R_{0p}^3 J}\int \mathrm{d}V \frac{\phi^{k-1}(\mathbf{r}')}{|\mathbf{r}-\mathbf{r}'|} = \frac{-e^2A}{R_{0p}J}\sum_\ell \frac{3\pi Y_{\ell 0}(\theta)}{4(2\ell+1)}\int_0^\pi \mathrm{d}\theta' \sin(\theta') Y^*_{\ell 0}(\theta') \times \left[\int_0^r \mathrm{d}r' \frac{(r')^{\ell+2}\phi^{k-1}(\mathbf{r}')}{r^{\ell+1}(R_{0p})^2} + \int_r^{R_{0p}f(\theta')} \mathrm{d}r' \frac{(r)^\ell \phi^{k-1}(\mathbf{r}')}{(r')^{\ell-1}(R_{0p})^2}\right], \quad (25)$$

which determines the potential with any necessary degree of accuracy. As a result, we can evaluate the volume and the surface contributions of the PEDM using eqs. (17), (18), (20), (24) and (25).

The macroscopic PEDM can be written as

$$D_{\mathrm{macro}} = D_{v1} + D_{v20} + D_{v21} + D_{s1} + D_{s20} + D_{s21}, \quad (26)$$

where

$$D_{v1} = \frac{e^3AZ}{\pi J}\left[\frac{9\beta_2\beta_3}{56\sqrt{35}} + \frac{11\beta_3\beta_4}{105\sqrt{7}} + \frac{41\beta_4\beta_5}{264\sqrt{11}} + \frac{441\beta_5\beta_6}{715\sqrt{143}}\right], \quad (27)$$

$$D_{s1} = \frac{15e^3A^{2/3}Z}{8\pi Q}\left[\frac{9\beta_2\beta_3}{56\sqrt{35}} + \frac{11\beta_3\beta_4}{105\sqrt{7}} + \frac{41\beta_4\beta_5}{264\sqrt{11}} + \frac{441\beta_5\beta_6}{715\sqrt{143}}\right] \quad (28)$$

are the volume and surface first-order contributions,

$$D_{v20} = \frac{e^3AZ}{\pi^{3/2}J}\left[\frac{3\beta_2^2\beta_3}{56\sqrt{7}} + \frac{789\beta_2^2\beta_5}{8624\sqrt{11}} + \frac{48721\beta_2\beta_3\beta_4}{101640\sqrt{35}} + \frac{65685\beta_2\beta_3\beta_6}{44044\sqrt{455}} + \frac{1658135\beta_2\beta_4\beta_5}{2186184\sqrt{55}} + \frac{35403\beta_2\beta_5\beta_6}{11440\sqrt{715}} + \frac{3\beta_3^3}{88\sqrt{7}} + \frac{19557\beta_3^2\beta_5}{104104\sqrt{11}} + \frac{27147\beta_3\beta_4^2}{220220\sqrt{7}} + \frac{657095\beta_3\beta_4\beta_6}{528528\sqrt{91}} + \frac{141723\beta_3\beta_5^2}{1041040\sqrt{7}} + \frac{110793\sqrt{7}\beta_3\beta_6^2}{5348200} + \frac{245625\beta_4^2\beta_5}{1457456\sqrt{11}} + \frac{46892\beta_4\beta_5\beta_6}{36465\sqrt{143}} + \frac{327\beta_5^3}{5746\sqrt{11}} + \frac{64461\beta_5\beta_6^2}{369512\sqrt{11}}\right], \quad (29)$$

$$D_{s20} = \frac{e^3A^{2/3}Z}{\pi^{3/2}Q}\left[\frac{297\beta_2^2\beta_3}{2240\sqrt{7}} + \frac{20277\beta_2^2\beta_5}{68992\sqrt{11}} + \frac{80181\beta_2\beta_3\beta_4}{54208\sqrt{35}} + \frac{2047545\beta_2\beta_3\beta_6}{352352\sqrt{455}} + \frac{16455195\beta_2\beta_4\beta_5}{5829824\sqrt{55}} + \frac{252207\beta_2\beta_5\beta_6}{18304\sqrt{715}} + \frac{81\beta_3^3}{704\sqrt{7}} + \frac{56025\beta_3^2\beta_5}{75712\sqrt{11}} + \frac{177669\beta_3\beta_4^2}{352352\sqrt{7}} + \frac{8432595\beta_3\beta_4\beta_6}{1409408\sqrt{91}} + \frac{1113129\beta_3\beta_5^2}{1665664\sqrt{7}} + \frac{1037259\sqrt{7}\beta_3\beta_6^2}{8557120} + \frac{9802305\beta_4^2\beta_5}{11659648\sqrt{11}} + \frac{299061\beta_4\beta_5\beta_6}{38896\sqrt{143}} + \frac{31455\beta_5^3}{91936\sqrt{11}} + \frac{3679965\beta_5\beta_6^2}{2956096\sqrt{11}}\right], \quad (30)$$

are the volume and surface second-order contributions related to the $\varphi^0(\mathbf{r})$ contribution (see eqs. (17), (18), (20), (24)), and

$$D_{v21} = -\frac{e^5A^{5/3}Z}{\pi J^2 r_0}\left[\frac{477\beta_2\beta_3}{15680\sqrt{35}} + \frac{3719\beta_3\beta_4}{194040\sqrt{7}} + \frac{176933\beta_4\beta_5}{6342336\sqrt{11}} + \frac{627219\beta_5\beta_6}{5725720\sqrt{143}}\right], \quad (31)$$

$$D_{s21} = -\frac{e^5A^{4/3}Z}{\pi JQ r_0}\left[\frac{459\beta_2\beta_3}{7840\sqrt{35}} + \frac{9623\beta_3\beta_4}{258720\sqrt{7}} + \frac{32881\beta_4\beta_5}{604032\sqrt{11}} + \frac{702081\beta_5\beta_6}{3271840\sqrt{143}}\right] \quad (32)$$

are the volume and surface second-order contributions connected to the $\varphi^1(\mathbf{r})$ contribution (see eqs. (17), (18), (19), (25)), $r_0 = R_{0p}/A^{1/3}$. This expression of the PEDM is obtained with the help of the symbolic computation software *Mathematica*.

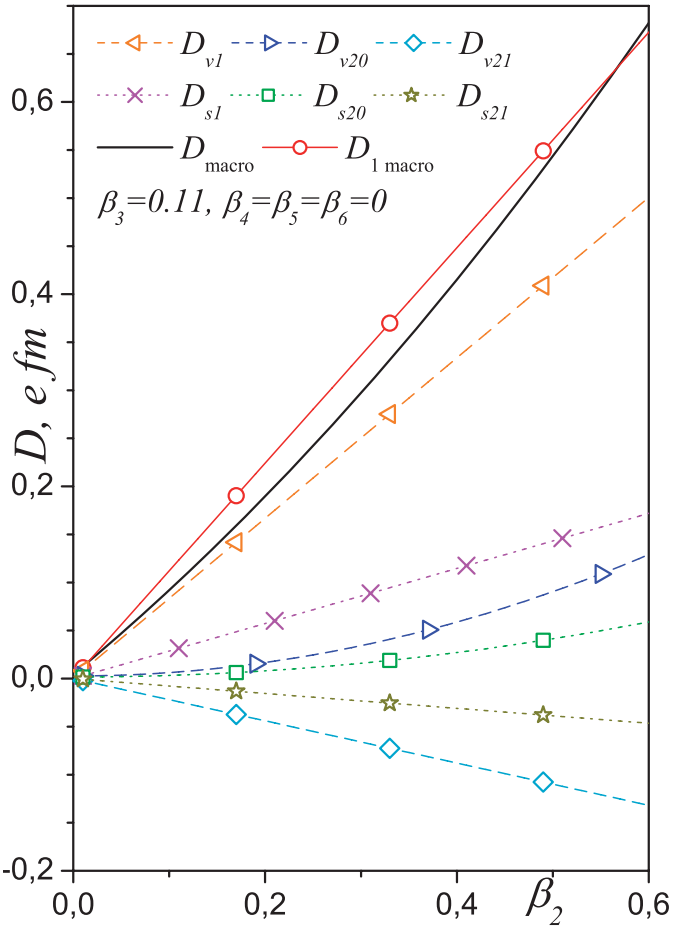

Fig. 2. Dependencies of the total macroscopic PEDM evaluated in the first $D_{1\rm macro}$ and second $D_{\rm macro}$ orders on the quadrupole β_2 deformation as well as the same dependencies of contributions D_{v1}, D_{v20}, D_{v21}, D_{s1}, D_{s20}, and D_{s21} to the PEDM. The quadrupole and octupole deformations of ^{220}Th are only taken into account.

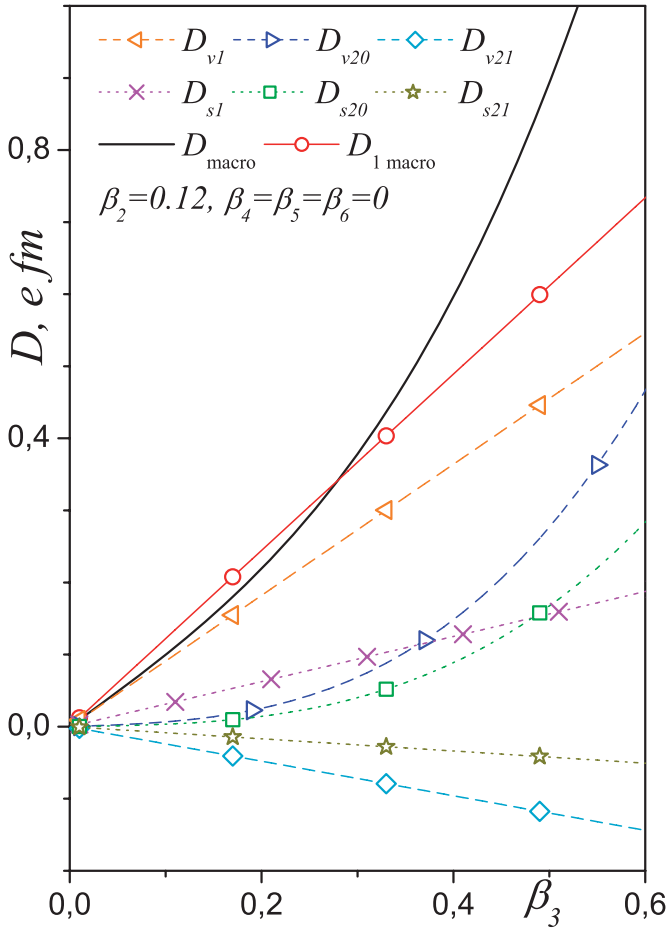

Fig. 3. Dependencies of the total macroscopic PEDM evaluated in the first $D_{1\rm macro}$ and second $D_{\rm macro}$ orders on the octupole β_3 deformation as well as the same dependencies of contributions D_{v1}, D_{v20}, D_{v21}, D_{s1}, D_{s20}, and D_{s21} to the PEDM. The quadrupole and octupole deformations of ^{220}Th are only taken into account.

We propose at evaluation of the PEDM that ratio of potentials $\varphi^1(\mathbf{r})/\varphi^0(\mathbf{r})$ is of the same order as β_ℓ, therefore we take into account terms proportional to the product of the deformations $\beta_\ell\beta_{\ell'}$ in D_{v21} or D_{s21} and neglect the next-order terms $\beta_\ell\beta_{\ell'}\beta_{\ell''}$. This proposal is natural for the hierarchy of solutions in the form of the perturbation series.

The first term in eq. (27) was obtained in refs. [1,3], eqs. (27) and (28) were derived in refs. [6,8], and eqs. (29)–(32) are found for the first time.

3 Discussion and conclusions

The total value of the PEDM, $D_{\rm tot}$, is the sum of the macroscopic, $D_{\rm macro}$, and the microscopic, $D_{\rm micro}$, shell-correction contributions [9,14,12] calculated for the same shapes of the proton and neutron surfaces [9], *i.e.*

$$D_{\rm tot} = D_{\rm macro} + D_{\rm micro}. \qquad (33)$$

The macroscopic part of the PEDM can be evaluated by using eqs. (26)–(32).

The total values of the PEDM evaluated in the framework of various models are compared with the experimental data for thorium isotopes in fig. 1. The experimental data are taken from refs. [13,25,26]. Our calculation of the macroscopic part $D_{\rm macro}$ is done with the help of eqs. (26)–(32) using the recent parameter values of the droplet model $J = 32.5\,$MeV, $Q = 29.4\,$MeV, $r_0 = 1.16$ [6]. The values of the multipole deformation parameters β_ℓ and the microscopic part of PEDM, $D_{\rm micro}$, are taken from ref. [14]. The results obtained in our model well agree with the experimental data for $^{220-228}$Th, see fig. 1. The total values of the PEDM calculated by Butler and Nazarewicz using the droplet model approach for the macroscopic part $D_{\rm tot\,BN} = D_{\rm macro\,DM} + D_{\rm micro}$ [14] are shown in fig. 1, too. The results of the droplet model approach underestimate the experimental data for $^{223-228}$Th, see fig. 1. The values of the PEDM obtained in the framework of the cranking Skyrme-Hartree-Fock approach $D_{\rm SHF}$ [15] are also pre-

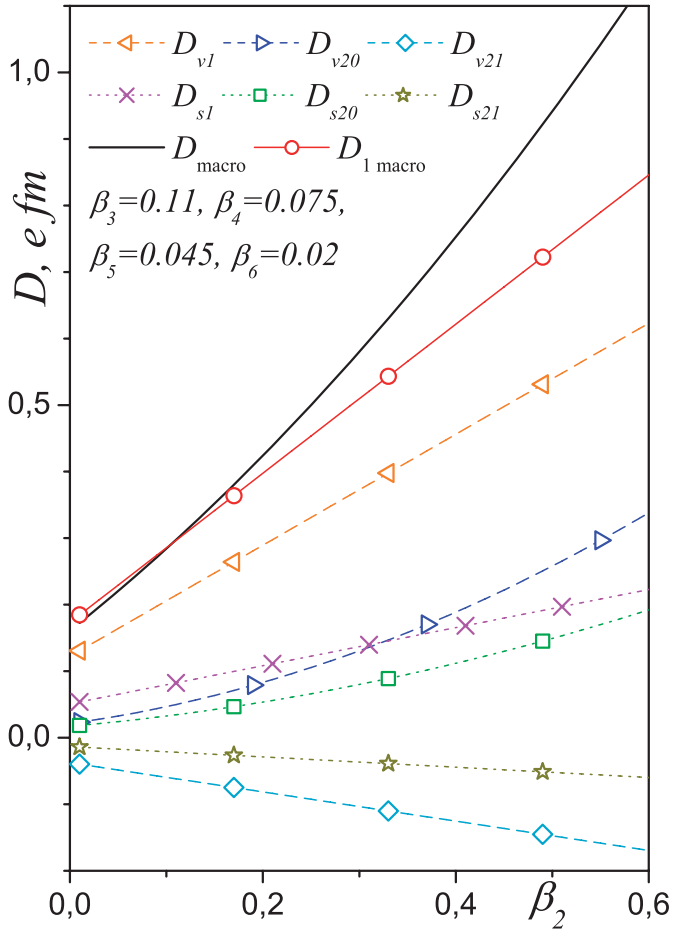

Fig. 4. The same as fig. 2, but taking into account also the high-order multipole deformations β_4, β_5 and β_6 of ^{220}Th.

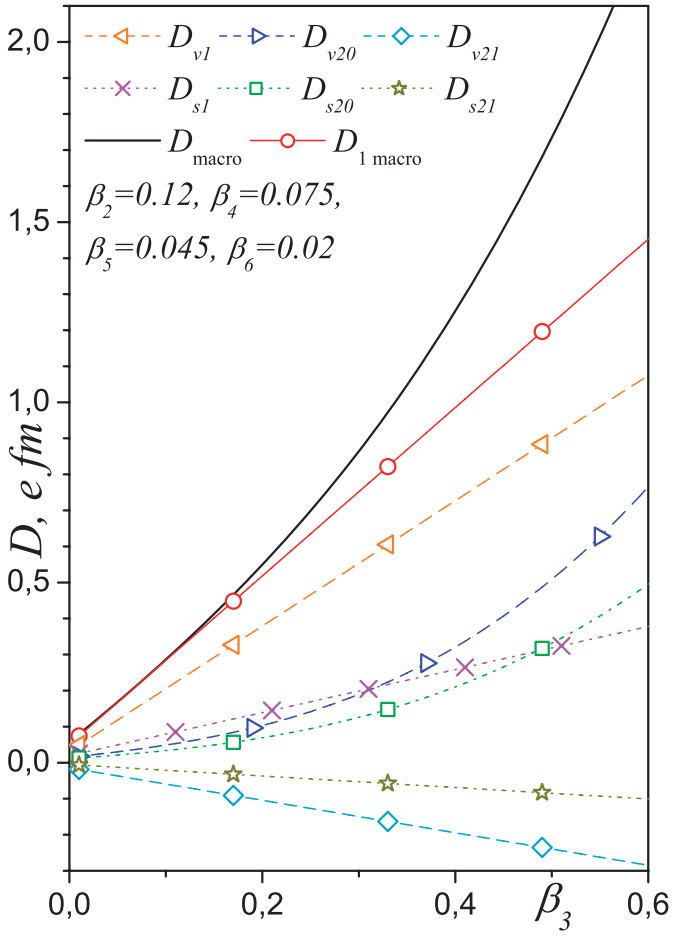

Fig. 5. The same as fig. 3, but taking into account also the high-order multipole deformations β_4, β_5 and β_6 of ^{220}Th.

sented in fig. 1. The values of the PEDM evaluated in the cranking Skyrme-Hartree-Fock model underestimate the experimental data for $^{222-227}$Th and overestimate the ones for ^{229,230}Th. The comparison of the PEDM values calculated in the framework of various models with the experimental data for thorium isotopes in fig. 1 suggest that our proposal, *i.e.* that the proton and neutron surfaces are geometrically similar (see eq. (2)), is reasonable.

The values of the macroscopic part of the PEDM evaluated in our model $D_{\rm macro}$ are larger than the ones obtained in the framework of the droplet model $D_{\rm macro\,DM}$, see fig. 1 and refs. [6–9]. Comparing the results in fig. 1 we conclude that the microscopic contribution to the PEDM $D_{\rm micro}$ is smaller than the macroscopic one $D_{\rm macro}$.

Let us study the role of second-order contributions in the macroscopic part of the PEDM in well-deformed nuclei. We consider first nuclei with quadrupole and octupole deformations. Here we neglect the microscopic part of the PEDM for simplicity. The dependence of the PEDM on the quadrupole deformation value at a fixed value of the octupole deformation is presented in fig. 2, while the dependence of the PEDM on the octupole deformation value at a fixed value of the quadrupole deformation is presented in fig. 3. Fixed values of quadrupole or octupole deformations are pointed out in figs. 2-3. These values of the deformation parameters are typical for the ground state of reflection asymmetric actinides [14].

The macroscopic PEDM consists of six contributions, D_{v1}, D_{v20}, D_{v21}, D_{s1}, D_{s20}, and D_{s21}, see eqs. (26)–(32). Contributions of all these terms to the PEDM as well as the total first- and second-orders macroscopic PEDM values are shown in figs. 2-3. Comparing the various lines in figs. 2-3 we conclude that:

- The total first-order contribution of the PEDM, $D_{1\rm macro} = D_{v1} + D_{s1}$, is mainly determined by the value of the PEDM at small values of the deformation parameters. The influence of the second-order terms rises with the values of the deformation parameters.
- Contributions D_{v1}, D_{s1}, $D_{1\rm macro}$, D_{v21}, and D_{s21} of the PEDM depend linearly on the variation of the deformation parameter β_2 or β_3 , while $D_{\rm macro}$, D_{v20} and D_{s20} depend quadratically on the variation of the deformation parameter β_2 or β_3.
- The surface contribution of any type is approximately twice as small than the volume contribution of the same type. (Note that this conclusion depends on the ratio between the values J and Q. We would like to

remind that we use the same values of J and Q as in the droplet model at the PEDM evaluation, but some authors [6,14,12] use other J and Q values to describe the PEDM experimental data.)

- The terms D_{v21} and D_{s21} related to the Coulomb potential correction φ^1 give negative contributions to the PEDM, while any other contribution is positive.
- The absolute values of the terms D_{v21} and D_{s21} are similar to the ones for the terms D_{v20} and D_{s20}. This supports our proposal on the hierarchy of solutions of the perturbation series.
- The contribution of the second-order terms $D_{v20} + D_{v21} + D_{s20} + D_{s21}$ gives a small correction for the case of variable quadrupole and fixed octupole deformations (see fig. 2). However this contribution noticeably enhances the value of the PEDM at large octupole deformation in the case of variable octupole and fixed quadrupole deformations (see fig. 3). The total PEDM evaluated at large octupole and fixed quadrupole deformations is larger than the one for large quadrupole and fixed octupole deformations.

Nuclei with reflection asymmetry have also non-zero values of high-order multipole deformations [12,14]. Dependencies of macroscopic PEDM on the value of the quadrupole and octupole deformation at fixed values of the other deformations are presented in figs. 4 and 5, respectively. Values of fixed high-order multipole deformations parameters pointed out in figs. 4-5 are typical for the ground state of reflection asymmetric actinides [14].

The values of high-order multipole deformations are smaller than the ones for quadrupole or octupole deformations as a rule [12,14]. Nevertheless, high-order multipole deformations enhance the value of the PEDM noticeably, compare results presented in figs. 2-5. The influence of second-order terms is also strengthened by high-order multipole deformations.

Qualitatively similar results related to the influence of second-order contribution on the PEDM were obtained numerically in ref. [12], but the contributions D_{v21} and D_{s21} related to φ^1 were skipped in this work. Note that Skalski [12] evaluated the macroscopic part of the PEDM for the case of constant neutron skin (the droplet model approach). As pointed out in the introduction, the PEDM evaluated in the framework of the droplet model has additional contribution related to the difference between the center of mass of the neutron skin of uniform thickness and the center of mass of the nucleus, which reduces the value of the PEDM induced by density redistribution [6], compare also lines denoted as $D_{\rm macro}$ and $D_{\rm macro\,DM}$ in fig. 1. This neutron skin contribution to the PEDM is zero in the case of neutron skin formed by geometrically similar neutron and proton surfaces. Therefore, numerical comparison of our and Skalski's results cannot show the difference between the first- and second-order contributions to the PEDM obtained in various approaches, because the comparison shows mainly the difference related to the neutron-skin contribution.

We evaluated the PEDM of the hyperdeformed state of ^{152}Dy. The values of the deformation parameters of ^{152}Dy in the hyperdeformed state are $\beta_2 = 0.61$, $\beta_3 = 0.1$, $\beta_4 = 0.11$, $\beta_5 = 0.05$ and $\beta_6 = 0$ [12]. The values of the macroscopic part of the PEDM obtained in the first and second orders using eqs. (26)–(32) are $D_{\rm macro} = 0.67\ e$ fm and $D_{\rm 1macro} = 0.46\ e$ fm, respectively. The microscopic shell-correction part of the PEDM evaluated for geometrically similar proton and neutron surfaces is $D_{\rm shell} = -0.34\ e$ fm [12]. As a result the total values of the PEDM found by applying the first- and second-order calculation of the macroscopic part of the PEDM are $D_{\rm macro}+D_{\rm shell} = 0.33\ e$ fm and $D_{\rm 1macro} + D_{\rm shell} = 0.12\ e$ fm, respectively. Note that the total value of the PEDM evaluated using the exact numerical calculation of the macroscopic contribution in the framework of the droplet model is $D_{\rm macro\,Skalski} + D_{\rm shell} = 0.06\ e$ fm [12]. Hereby, the PEDM depends strongly on the second-order terms in well-deformed nuclei as well as on the neutron skin shape.

In conclusion, the expression for macroscopic PEDM taking into account the first- and second-order terms in the parameters of multipole deformations is obtained in the case of geometrically similar proton and neutron surfaces of reflection asymmetric nuclei.

The second-order terms are important at large values of the deformation parameters. The second-order terms are especially important for the nuclear shape with non-zero values of high-order multipole deformation parameters.

The second-order contributions D_{v20} and D_{s20} enlarge the value of the PEDM obtained in the first order. In contrast to this, contributions D_{v21} and D_{s21} decrease the value of the PEDM obtained in the first order. Compensation of these contributions into the PEDM value occurs at small deformation values. However the contribution $D_{v20} + D_{s20}$ to the PEDM value is larger than contributions $D_{v21} + D_{s21}$ at large values of the deformation parameters.

The reduced probabilities of dipole transitions $B(E1)$ are measured in various experiments [13,22–26]. Note that $B(E1)$ is proportional to the squared value of the PEDM D^2 [13,17–21]. Therefore, the second-order contribution to the PEDM leads to significant variation of $B(E1)$ in well-deformed nuclei.

The obtained expression can be easily applied for the estimation of the macroscopic PEDM and strength of dipole transition probabilities in various well-deformed nuclei.

The author thanks Prof. F.F. Karpeshin for stimulating discussions.

References

1. V.M. Strutinsky, At. Energ. **4**, 150 (1956) (in Russian); J. Nucl. Energy **4**, 523 (1957) (English translation).
2. A. Bohr, B.R. Mottelson, Nucl. Phys. **4**, 529 (1957).
3. A. Bohr, B.R. Mottelson, Nucl. Phys. **9**, 687 (1958).
4. P.O. Lipas, Nucl. Phys. **40**, 629 (1963).

5. D.P. Leper, Izv. AN SSSR. Ser. Fiz. **29**, 1253 (1965).
6. C.O. Dorso, W. Myers, W. Swiatecki, Nucl. Phys. A **451**, 189 (1986).
7. W. Myers, W. Swiatecki, Nucl. Phys. A **531**, 93 (1991).
8. V.Yu. Denisov, Yad. Fiz. **49**, 644 (1989) (Sov. J. Nucl. Phys. **49**, 399 (1989)).
9. V.Yu. Denisov, Yad. Fiz. **55**, 2647 (1992) (Sov. J. Nucl. Phys. **55**, 1478 (1992)).
10. V.Yu. Denisov, O.I. Davidovskaya, Yad. Fiz. **59**, 981 (1996) (Phys. At. Nucl. **59**, 981 (1996)).
11. J. Skalski, Phys. Rev. C **43**, 140 (1991).
12. J. Skalski, Phys. Rev. C **49**, 2011 (1994).
13. P.A. Butler, W. Nazarewicz, Rev. Mod. Phys. **68**, 350 (1996).
14. P.A. Butler, W. Nazarewicz, Nucl. Phys. A **533**, 249 (1991).
15. A. Tsvetkov, J. Kvasil, R.G. Nazmitdinov, J. Phys. G **28**, 2187 (2002).
16. L.M. Robledo, M. Baldo, P. Schuck, X. Vinas, Phys. Rev. C **81**, 034315 (2010).
17. A.Ya. Dzyublik, V.Yu. Denisov, Yad. Fiz. **56**, 30 (1993) (Phys. At. Nucl. **56**, 303 (1993)).
18. V.Yu. Denisov, A.Ya. Dzyublik, Yad. Fiz. **56**, 96 (1993) (Phys. At. Nucl. **56**, 477 (1993)).
19. V.Yu. Denisov, A.Ya. Dzyublik, Nucl. Phys. A **589**, 17 (1995).
20. N. Minkov *et al.*, Phys. Rev. C **76**, 034324 (2007).
21. A.A. Raduta, C.M. Raduta, A. Faessler, Phys. Rev. C **80**, 044327 (2009).
22. T. Rzaca-Urban *et al.*, Phys. Rev. C **82**, 017301 (2010).
23. S.H. Liu *et al.*, Phys. Rev. C **81**, 057304 (2010).
24. S.S. Ntshangase *et al.*, Phys. Rev. C **82**, 041305(R) (2010).
25. N.J. Hammond *et al.*, Phys. Rev. C **65**, 064315 (2002).
26. K. Gulda *et al.*, Nucl. Phys. A **703**, 45 (2002).
27. F.F. Karpeshin, Z. Phys. **344**, 55 (1992).
28. F.F. Karpeshin, Eur. Phys. J. A **45**, 251 (2010).
29. F.F. Karpeshin, *Proceedings of the 3rd International Conference on Nuclear Physics and Atomic Energies, June 2010, Kyiv* (Institute for Nuclear Research, Kyiv, 2011) p. 441.
30. F.F. Karpeshin, *Proceedings 41-42 Winter Schools of St.-Petersburg's Institute of Nuclear Physics*, (Institute of Nuclear Physics, St.-Petersburg, 2008) p. 216.
31. B. Crowell *et al.*, Phys. Rev. C **51**, R1599 (1995).
32. A.N. Wilson *et al.*, Phys. Rev. C **54**, 559 (1996).
33. T. Nakatsukasa *et al.*, Phys. Rev. C **53**, 2213 (1996).
34. A. Korichi *et al.*, Phys. Rev. Lett. **86**, 2746 (2001).
35. J. Kvasil *et al.*, Phys. Rev. C **75**, 034306 (2007).
36. M. Kowal, J. Skalski, Phys. Rev. C **82**, 054303 (2010).
37. A. Bohr, B. Mottelson, *Nuclear Structure*, Vol. **II**, (Benjamin, N.Y., 1975).
38. V.G. Soloviev, *Theory of Complex Nuclei* (Pergamon, Oxford, 1976).
39. P. Ring, P. Schuck, *The Nuclear Many-Body Problem* (Springer, Berlin, 1980).
40. S. Cwiok, J. Dudek, W. Nazarewicz, J. Skalski, T. Werner, Comput. Phys. Commun. **46**, 379 (1987).
41. S.G. Nilsson, I. Ragnarsson, *Shapes and Shells in Nuclear Structure* (Cambridge University Press, Cambridge, 1995).
42. Y. Aboussir, J.M. Pearson, A.K. Dutta, At. Data Nucl. Data Tabl. **61**, 127 (1995).
43. A. Baran, Z. Lojewski, K. Sieja, M. Kowal, Phys. Rev. C **72**, 044310 (2005).
44. M. Kowal, P. Jachimowicz, A. Sobiczewski, Phys. Rev. C **82**, 014303 (2010).
45. J.F. Berger, K. Pomorski, Phys. Rev. Lett. **85**, 30 (2000).
46. A. Dobrowolski, K. Pomorski, J. Bartel, Phys. Rev. C **65**, 041306(R) (2002).
47. A. Trzcinska *et al.*, Phys. Rev. Lett. **87**, 082501 (2001).
48. A. Trzcinska, Acta Phys. Polonica B **41**, 311 (2010).